IAC-22-C2.9.6.x69344

Self-healing polymers for space: a study on autonomous repair performance and response to space radiation

Laura Pernigoni[a]*, Ugo Lafont[b], Antonio M. Grande[a]

[a] *Department of Aerospace Science and Technology, Politecnico di Milano, via La Masa 34,20156 Milan, Italy*, laura.pernigoni@polimi.it, antoniomattia.grande@polimi.it
[b] *European Space Research and Technology Centre, European Space Agency, Keplerlaan 1, PO Box 299, 2200 AG Noordwijk, The Netherlands*, ugo.lafont@esa.int
* Corresponding Author

Abstract

One of the main challenges of space exploration is to design novel light, initially packed structures that both make the best use of the reduced transport capacity of the available launchers and ensure safety and reliability levels comparable to those of classical solutions. For this reason, space inflatable structures have recently gained interest: initially folded in stowed configuration to fit in the launcher's space dedicated to the payload, they can be then inflated and deployed to reach the required volume. In addition, these structures are much lighter than traditional ones and would significantly reduce the related mission costs.

However, these solutions are currently unable to withstand damage after, for example, impacts with micrometeoroids and orbital debris (MMOD), and they would depressurise and collapse if punctured, with catastrophic consequences for devices and astronauts in case of crewed missions. In this context, the possibility of integrating self-healing materials into inflatable and deployable space structures has drawn the attention of the scientific community, as it would lead to autonomous damage restoration and subsequently increased spacecraft safety, operational life, and autonomy. Nevertheless, the effects of space environment on these materials are still to be determined and could lead to a significant decrease of their overall performance.

The here presented study analyses the healing performance of a set of candidate self-healing polymers for space applications (either studied as matrices into nanocomposites or inserted into multilayers) as well as its variation after irradiation under simulated space radiation.

The self-healing response is assessed through in-situ flow rate measurements after puncture damage. Maximum and minimum flow rate, the time between them and the air volume lost within the 3 minutes following puncture are collected as healing performance parameters. The same tests are then repeated on gamma-ray irradiated samples to study the variation in self-repairing performance after exposure to simulated space radiation. Results show that the healing performance is higher in systems with lower viscous response, and that this performance decreases in the irradiated samples. A further analysis of the effects of space environment on the presented materials is hence required. The NASA HZETRN2015 (High Z and Energy TRaNsport, 2015 version) software is also used to simulate galactic cosmic rays. The materials are compared to identify the most promising candidates, and possible solutions to increase their shielding performance are considered.

Keywords: self-healing polymers, space radiation, composites, inflatable space structures

Nomenclature

Q: ICRP-60 quality factor
Q_{max}: maximum flow rate after puncture test
Q_{min}: minimum flow rate after puncture test
S_j: stopping power of a particle j
V_{leak}: volume leaked within 180 s after puncture
Δt: time between Q_{max} and Q_{min}
φ: solar modulation parameter

Acronyms/Abbreviations

CNT: carbon nanotubes
DGEBA: diglycidyl ether of bisphenol A
GCR: galactic cosmic rays
HZETRN2015: High Z and Energy TRaNsport, 2015 version
MI: Methyl Imidazole
MMOD: micrometeoroids and orbital debris
MWCNT: multiwalled carbon nanotubes
PUU: polyurea-urethane
SPE: solar particle event

1. Introduction

Inflatable and deployable structures are being considered in the framework of future space missions, as they would ensure reduced mass and launch cost due to their light weight and high packing efficiency [1]. Nevertheless, their structural integrity might be compromised by environmental factors such as vacuum, atomic oxygen, radiation, and micrometeoroids and orbital debris (MMOD). In particular, as these structures

typically have low mechanical properties, possible cuts and punctures generated by impacts with MMOD could lead to their depressurization, a significant and eventually fatal issue for long-term crewed missions [2]. An effective solution to enhance the lifetime and safety of future spacecraft could be the insertion of self-healing polymers, but their properties could in turn be strongly modified by the space environment [3]. An example is given by possible degradation due to exposure to ionizing radiation from Galactic Cosmic Rays (GCR), Solar Particle Events (SPE) and Van Allen Belts [4]. Radiation must be contrasted through shielding due to its detrimental effects on material performance as well as human health. In particular, even if their effects on polymers in space still need to be fully determined, it was observed that GCR can change puncture extension and ultimate tensile strength, and decrease ballistic performance as well as load-bearing capacity [5]. These aspects must hence be considered in the planning of future space missions [3,6], which might rely on multifunctional materials with combined self-healing and radiation shielding properties.

The aim of the here presented work is to experimentally characterize the self-healing performance of polyurea-urethanes (PUUs) and a supramolecular polymer with intrinsic autonomic self-healing properties, and to perform a preliminary study of the effects of simulated space radiation on these polymers both through irradiation tests and software tools.

The first part of this research focuses on puncture tests as a preliminary representation of MMOD impacts, analyzing their effect on different samples [2]. Multilayer and nanocomposite samples are investigated alongside reference neat polymer specimens. After the initial puncture tests, some of the promising specimens are exposed to 100 Gy radiation doses before being tested again. A comparison is then made between pre and post irradiation results, to assess the possible changes of healing performance after exposure to radiation.

Finally, the NASA HZETRN2015 (High Z and Energy TRaNsport, 2015 version) software is used to simulate GCR and have an initial idea about if and to what extent the considered solutions can shield space radiation. The results are expressed in terms of absorbed equivalent dose as a function of the material's depth. Some of the neat materials are initially compared to find the ones with the best intrinsic properties, and then an attempt to further increase shielding is performed through insertion of nanofillers. Here GCR simulations are performed again, and the contribution of the nanofillers to the shielding properties is evaluated.

2. Materials and methods

2.1 Self-healing polymers

Four PUUs with similar formulation and fixed disulphide content but different crosslinking densities are analyzed (Table 1). They are obtained from different combinations of trifunctional and difunctional isocyanate-terminated pre-polymers PU-6000 and PU-4000, organized into networks connected by aromatic disulphides linkages and containing urea related H-bonds [7]. These pre-polymers are obtained from the interaction between poly(propylene glycol) and isophorone diisocyanate in the presence of the dibutyltin dilaurate catalyst [8].

Table 1 : PUUs formulations and basic properties [7].

Sample	Composition* [wt%]		ν [10^{-4} mol/cm^3]	T_g [°C]
PUU	PU-6000	PU-4000		
100	93.8	0	2.35	-58.8
90	84.4	9.4	2.05	-59
80	75.1	18.7	1.77	-59.4
70	65.7	28.1	1.50	-60.1

* Linker wt%: 6.2

The supramolecular polymer Reverlink® is also considered. It contains both covalent bonds and supramolecular hydrogen-bonding crosslinks (50:50 mol%). It is obtained from the combination of supramolecular pre-polymer SP-50, diglycidyl ether of bisphenol A (DGEBA) resin and 2-Methyl Imidazole (2-MI) catalyst, with nominal proportions reported in Table 2 [9,10]. The non-cured material is heated to 90 °C, poured into a Teflon® mold and then cured at temperatures in the 120-150 °C range. Its glass transition temperature is between 5 °C and 15 °C [11,12]. For the sake of simplicity, this material will be from now on indicated with the HN-50 label.

Table 2 : Reverlink® (HN-50) components [9].

Component	SP-50	DGEBA	2-MI
Mass [g]	23.900	6.020	0.004

2.2 Nanocomposites and multilayers

Nanocomposites with self-healing polymeric matrix and Nanocyl® NC7000™ multiwalled carbon nanotubes (MWCNTs) [13] are considered as they could reduce the dose of incoming radiation reaching the interiors of a

spacecraft. A trade-off between radiation shielding and self-healing behavior is looked for, as the insertion of nanofillers usually decreases the healing performance.

Multilayer solutions are also analyzed to investigate possible healing performance improvements given by coupling the polymers with an additional layer (a 0.63 mm-thick aramid fabric or a 1.6 mm-thick silicone elastomer).

2.3 Samples manufacturing and puncture tests

Examples of specimens are shown in Figure 1. The HN-50 samples have a nominal diameter of 60 mm and variable thickness, while the PUU ones have a nominal diameter of 20 mm.

In the aramid/HN-50 configuration the resin is poured on top of the aramid fibers, while for the other multilayers the already cured polymers are re-heated and coupled with the elastomer by applying pressure on the layers. 1 mm-thick polymeric layers are used in the PUU multilayer case. For the sake of clarity, the elastomer/HN-50 multilayer will be here indicated with the ME label.

As concerns the nanocomposites, in the experimental phase only samples with HN-50 matrix are manufactured and tested. The MWCNTs are inserted into this polymer with weight concentrations from 0.1% to 1%.

(a) (b) (c) (d)

Figure 1: Specimens examples - (a) Neat polymer, (b) nanocomposite and (c)(d) multilayers.

All samples are treated with a 24-hour drying cycle to remove humidity and then inserted between two polyamide films. This configuration is mounted on a system used to evaluate the self-healing performance through puncture tests and subsequent acquisition of the resulting leakage flow rate (Figure 2). The samples are fixed on the central cylindrical part of the device and pressurized to a relative pressure of 30 kPa. Continuous air supply is provided to reproduce the reference case study represented by the internal environment of a space suit. A vertical sinusoidal motion is imposed to the puncheon by the MTS 858 Mini Bionix® II machine (Figure 3). An amplitude of 9.62 mm and 0.14 Hz frequency are set to obtain a velocity of 8.467 mm/s when the puncheon penetrates the specimen, coherently with the ASTM F1342/F1342M-05 standard. Each specimen is tested three times, and maximum and minimum flow rates, the time between them and the air volume lost within 3 minutes from the puncturing event are collected as self-healing performance indicators.

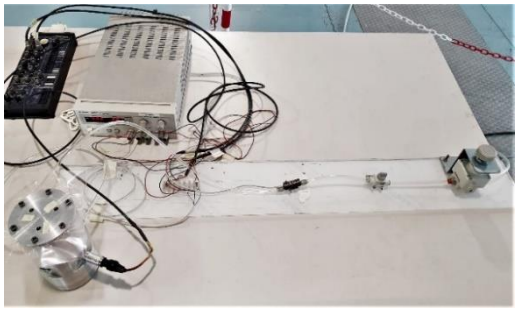

Figure 2: Testing system.

Figure 3: MTS 858 Mini Bionix® II machine for puncture tests.

2.4 Experimental setup for irradiation

Undamaged neat PUU samples are exposed to 100 Gy radiation doses emitted at 11.1 Gy/min rate by a Cobalt-60 source placed at a distance of 60.96 cm from the target. The irradiation process is performed in air, and the samples are subsequently stored in a cold room until the time of puncture tests to preserve chemical bonds deterioration generated by exposure to gamma rays.

2.5 Numerical irradiation simulations

An initial comparison of neat PUU 100, chosen as a reference for the PUUs family, and HN-50 is followed by the analysis of nanocomposites compared to an aramid fabric/HN-50 multilayer, as described in more detail in sub-subsections 2.5.1 and 2.5.2. In both cases high density polyethylene (HDPE) is used as a benchmark due to its known shielding ability [14].

The HZETRN2015 software tool [15] is used to simulate irradiation of the analysed materials under solar minimum conditions (maximum GCR intensity, low probability of SPE occurrence). A slab geometry with normally incident environment boundary conditions is considered for the materials.

2.5.1 Neat polymers

In the first set of simulations neat PUU 100 and HN-50 are irradiated with GCR in solar minimum conditions (φ = 400 MV). The related curves of proton and alpha equivalent doses are analysed. A single-layer slab geometry with a thickness of 200 g/cm^2 and 21 equally spaced target points is considered.

2.5.2 Nanocomposites

The responses to radiation of nanocomposites with HN-50 and PUU 100 matrices and different MWCNT contents are studied and compared to find the filler's concentration leading to the highest overall performance and its correlation with the shielding properties.

The 1%, 5% and 10% CNT weight percentages are analysed, keeping in mind the 20% upper threshold dictated by practical limitations while processing the composites [14]. The aramid fabric/HN-50 double layer configuration is also considered.

As in the neat case, the absorbed equivalent doses of protons and alpha particles from GCR exposure in solar minimum conditions are obtained and compared. The total thickness of the materials is set to 200 g/cm^2, with the bilayer configuration characterised by an external aramid layer with 59.7 g/cm^2 thickness and an internal HN-50 layer with 140.3 g/cm^2 thickness.

3. Theory and calculation

3.1 GCR simulations

As regards the simulation of GCR in HZETRN2015, the updated Badhwar-O'Neill model is used to generate the spectra of the related ions [16]. The solar modulation parameter φ is chosen as an input and set to 400 MV (solar minimum).

To assess the stochastic effects of radiation on the human body (such as cancer mortality and genetic damage) the equivalent doses of protons and alpha particles are the chosen outputs of the simulations as these are fundamental components of space radiation. The absorbed doses in Gy are converted into equivalent doses in Sv through the quality factor Q. This factor is a function of S_j (Eq. 1) [17]:

$$Q = \begin{cases} 1 & 0 < S_j \leq 10 \\ 0.32S_j - 2.2 & 10 < S_j \leq 100 \\ \dfrac{300}{\sqrt{S_j}} & S_j > 100 \end{cases} \quad (1)$$

The equivalent dose per day is analysed as a function of the material depth, considering that for the same thickness lower absorbed doses are related to better shielding performance [17]. Thicknesses are indicated in g/cm^2 (cumulative areal density), as usually done in radiation analysis.

4. Results and discussion

4.1 Puncture tests on non-irradiated samples

Focusing on the nanocomposite samples, the puncture tests show that self-healing is mainly related to the specimen's thickness rather than to the concentration of MWCNTs. Furthermore, complete healing is not reached, and practical issues are also encountered when trying to increase the concentration of nanotubes, making this solution less appealing than the multilayers. For the sake of clarity, Figure 4 shows the experimental data for the 1% MWCNT configuration as a reference example.

As concerns the multilayer configurations, while the aramid fabric does not provide significant improvements the polymer/elastomer coupling on the other hand increases the self-healing performance. As a matter of fact, the elastomer's springback behavior accelerates the self-healing process by promoting hole closure in the punctured region (Figure 5, Figure 6). The multilayer configuration containing the PUU 90 polymer is characterized by the highest average performance (

Table 3), which is in contrast with the neat polymers results. In the neat configuration PUU 100 has in fact the best overall performance, probably due to its strong springback response which ensures short healing times and reduced air leakage after perforation. This discrepancy between the multilayer and neat cases might be due to repeatability issues in the experiments and needs to be further investigated.

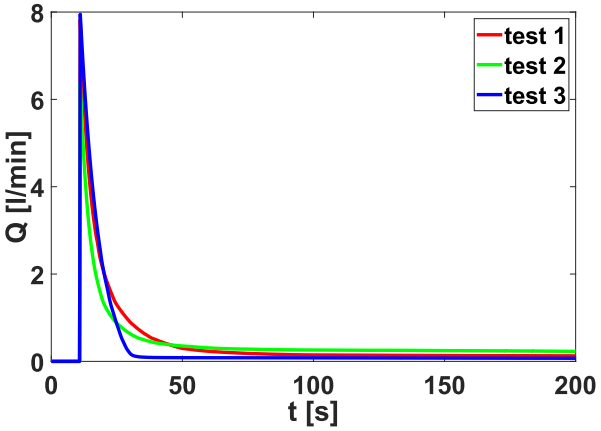

Figure 4: Puncture test results for the MWCNT nanocomposite with HN-50 matrix.

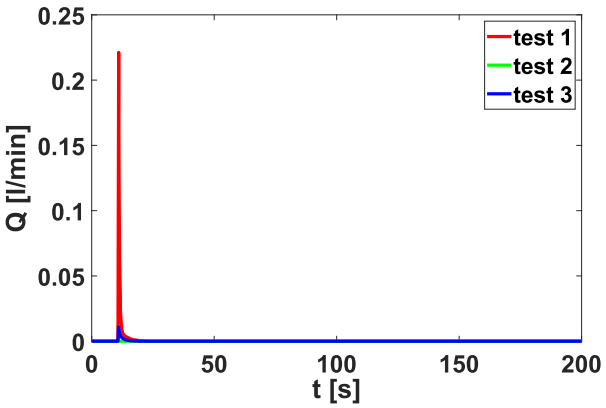

Figure 5: Puncture test results for the ME configuration (HN-50/elastomer multilayer).

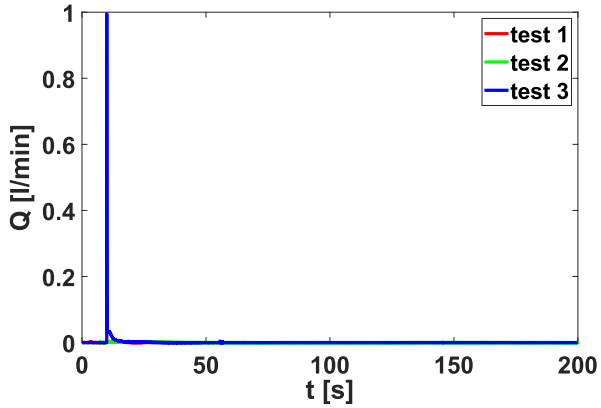

Figure 6: Puncture test results for the PUU 100-elastomer multilayer.

Table 3 : Average results obtained for elastomeric multilayer and nanocomposite specimens.

Sample	Q_{max} [l/min]	Q_{min} [l/min]	Δt [s]	V_{leak} [l]
Multilayer with elastomer				
ME	0.0777	0	7.96	0.0005
PUU 70	0.4017	0	99.62	0.0059
PUU 80	0.1860	0	11.44	0.0020
PUU 90	0.0411	0	9.08	0.0004
PUU 100	0.3352	0	10.47	0.0012
Nanocomposite				
1% CNT	7.3830	0.1423	200.00	1.2519

4.2 Puncture tests on irradiated samples

Comparison of average results for irradiated and blank (non-irradiated) PUU samples of the same type and thickness shows that deterioration of the healing performance is already visible under for a dose of 100 Gy. In general, stronger degradation is observed in materials with larger difunctional units contents. The neat PUU 100 samples results are displayed as a reference example in Table 4 and Figure 7.

Table 4 : Puncture tests results for irradiated and non-irradiated neat PUU 100 samples.

Sample	Q_{max} [l/min]	Q_{min} [l/min]	Δt [s]	V_{leak} [l]
Irradiated				
1	2.8231	0.0281	189.69	0.1453
2	3	0.0171	189.57	0.1003
3	2.6221	0.0503	188.61	0.2861
Non irradiated				
1	1.2549	0	5.66	0.0025
2	1.7352	0.0147	189.80	0.1057
3	1.5489	0	4.84	0.0017

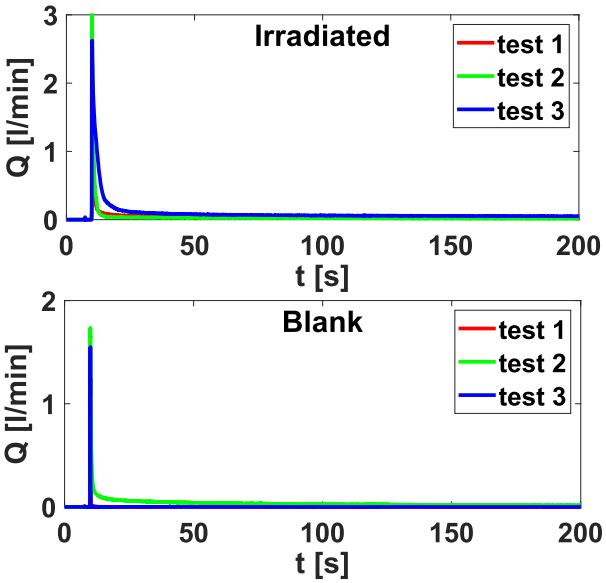

Figure 7: Puncture tests comparison for irradiated and blank (non-irradiated) neat PUU 100 samples.

4.3 Simulated irradiation on neat polymers

Figure 8 and Figure 9 show the comparison of the results from simulated GCR irradiation of the neat polymers. Being the shielding properties similar within the different PUUs, for the sake of clarity PUU 100 is chosen as the representative material and only the dose curves related to it are displayed in the plots.

As materials absorbing a lower dose for the same thickness are better in terms of radiation shielding [15], PUUs have a higher performance with respect to HN-50, but the reference material HDPE nevertheless remains the one with the best shielding ability.

A general objection that could be made is that at a given cumulative areal density the equivalent thickness in cm is higher for materials with lower density, hence the equivalent dose is larger and the curve moves rightwards [17]. Being the densities of the considered materials similar, though, the dose-versus-areal density curves can be directly used to compare them.

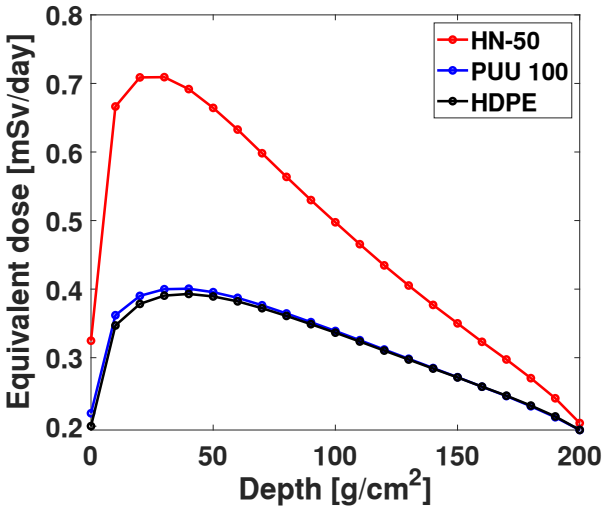

Figure 8: Protons equivalent doses, neat case.

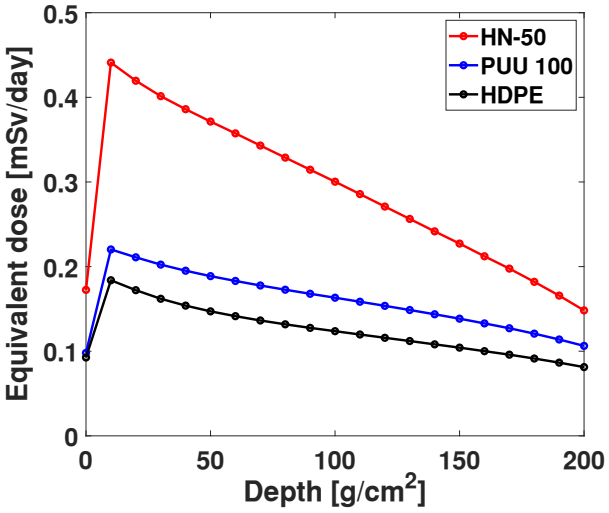

Figure 9: Alpha particles equivalent doses, neat case.

4.4 Simulated irradiation on nanocomposites

The results of the HZTERN2015 simulations show an initial growth in the equivalent dose due to the secondary radiation arising from the interaction of the materials with GCR. The protons equivalent dose curves all peak between 25 and 40 g/cm^2, while for the alpha particles the increasing trend stops around 10 g/cm^2 (Figure 10, Figure 11). The best results are related to the PUU 100 composites up to approximately 90 g/cm^2 in the protons case and slightly after 150 g/cm^2 for alpha particles. Moving to higher thicknesses the nanocomposites are surpassed by the aramid/HN-50 multilayer.

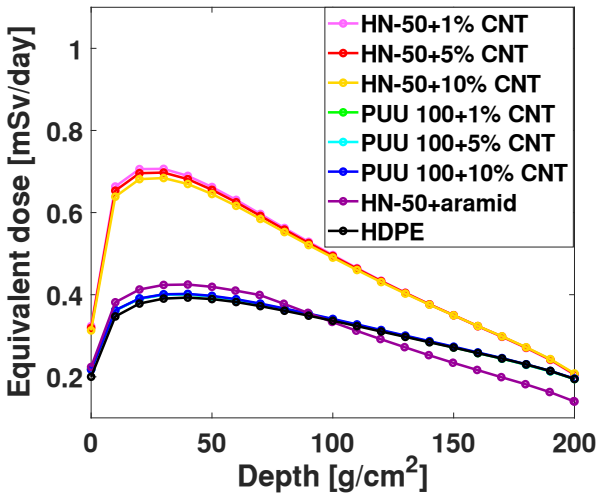

Figure 10: Protons equivalent doses, nanocomposites.

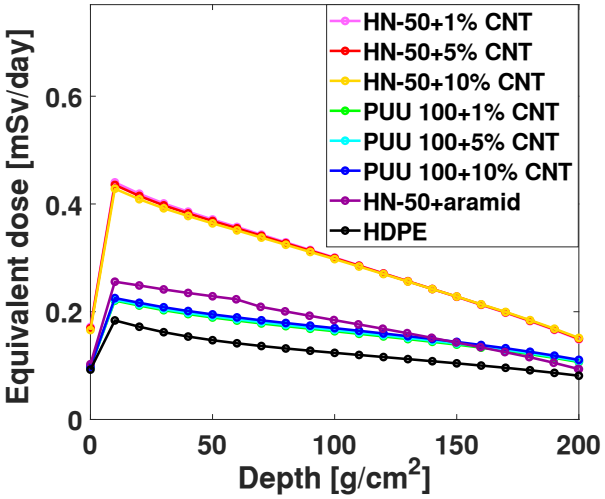

Figure 11: Alpha particles equivalent doses, nanocomposites.

A general improvement is observed in the HN-50 nanocomposites when increasing the filler concentration, leading to lower absorbed equivalent doses. Even if the addition of MWCNTs is usually expected to decrease the shielding performance through the reduction of hydrogen atoms in the matrix [14], in this case it actually has a positive effect on HN-50, because it reduces the concentration of heavier nitrogen and oxygen atoms and increases that of lighter carbon atoms. In any case, the radiation shielding ability of the HN-50 composites remains quite below that of HDPE, and a way better

response is observed in the aramid/HN-50 multilayer and in the PUU 100 composites. When comparing the neat and composite PUU 100 cases, though, it is noticed that inserting nanofillers into PUU 100 does not lead to relevant improvements to the polymer's radiation shielding performance. In the studied case the high cost, complexity and manufacturing challenges related to the nanocomposites lead to the idea of discarding them in favour of the much more affordable and easier to implement multilayer or neat PUU 100 configurations.

5. Conclusions

The presented work experimentally evaluates the self-healing performance before and after gamma-ray radiation of a set of self-healing polymers for possible space applications and gives an estimation of the radiation equivalent doses absorbed by these materials. It also studies the outcome of a CNT insertion method in terms of shielding performance improvement.

The puncture tests phase shows that the polymer/elastomer layer coupling leads to significant improvements with respect to previous studies, and this configuration can be optimized through a trade-off between thickness reduction and preservation of the self-healing properties. Furthermore, optimal healing performance could be ensured in the neat materials by a good trade-off between elastic and viscous behavior, as the former allows fast contact between the edges of a damaged area, and the latter is required for sealing. Overall, the most promising solution is the multilayer configuration coupling the elastomer with PUU 90.

As concerns the effects of space radiation, even limited doses of the order of 100 Gy can already compromise the materials' healing performance.

The HZETRN2015 simulations from the last part of this study show that PUU 100 has the highest overall shielding performance among the neat polymers but is nevertheless unable to surpass the baseline material HDPE. The subsequent insertion of nanofillers into HN-50 effectively increases its radiation shielding ability, but this remains relatively low. On the other hand, the benefits given to PUU 100 by adding nanofillers are not relevant. It is hence chosen to stick with the more convenient and affordable multilayer or PUU 100 neat solutions.

As a general conclusion, a self-healing layer could indeed significantly increase safety, reliability, and lifetime of spacecraft for future missions, but further studies must be carried out to successfully implement this solution.

As a future step, the here used slab geometry approach could be replaced by 3D numerical analysis to obtain more accurate results. To get an initial estimate of the operational life of the materials, a complete mission should also be simulated to analyse the doses absorbed by a multilayer space structure with an integrated self-healing layer at each mission phase (e.g.: EVAs, transfer route, permanence on the surface of a planet or satellite).

Finally, another important and necessary step is the experimental characterisation of specimens of part of the analysed materials under simulated space radiation environment to analyse how their mechanical, self-healing, chemical and physical properties degrade in space.

Acknowledgements

This research was supported by ESA, contract No. 4000132669/20/NL/MH/ic. The authors are grateful to Arkema for supplying Reverlink®, and to Prof. Mario Mariani and the Radiochemistry and Radiation Chemistry Laboratory at Politecnico di Milano for the help with the irradiation tests. Special thanks go to Alberto Sironi for the help provided with the HZETRN2015 tool.

References

[1] D. Cadogan, C. Scheir, A. Dixit, J. Ware, E. Cooper, P. Kopf, Intelligent Flexible Materials for Deployable Space Structures (InFlex), in: 47th AIAA/ASME/ASCE/AHS/ASC Struct. Struct. Dyn. Mater. Conf., AIAA, Newport, 2006. https://doi.org/10.2514/6.2006-1897.

[2] L. Pernigoni, A.M. Grande, Development of a supramolecular polymer based self-healing multilayer system for inflatable structures, Acta Astronaut. 177 (2020) 697–706. https://doi.org/10.1016/j.actaastro.2020.08.025.

[3] L. Pernigoni, U. Lafont, A.M. Grande, Self-healing materials for space applications: overview of present development and major limitations, CEAS Sp. J. (2021). https://doi.org/10.1007/s12567-021-00365-5.

[4] J. Rask, W. Vercoutere, B.J. Navarro, A. Krause, Space faring: the radiation challenge, an interdisciplinary guide on radiation and human space flight, (2008).

[5] J.M. Waller, K. Rojdev, K. Shariff, D.A. Litteken, R.A. Hagen, Simulated Galactic Cosmic Ray and Solar Particle Event Radiation Effects on Inflatable Habitat , Composite Habitat , Space Suit and Space Hatch Cover Materials, 2020.

[6] S.K. Ghosh, ed., Self-healing materials-Fundamentals, design strategies, and applications, Wiley-VCH, 2009.

[7] A.M. Grande, R. Martin, I. Odriozola, S. van der Zwaag, S.J. Garcia, Effect of the polymer structure on the viscoelastic and interfacial healing behaviour of poly(urea-urethane) networks containing aromatic disulphides, Eur. Polym. J. 97 (2017). https://doi.org/10.1016/j.eurpolymj.2017.10.007

.

[8] A. Rekondo, R. Martin, A. Ruiz de Luzuriaga, G. Cabañero, H.J. Grande, I. Odriozola, Catalyst-free room-temperature self-healing elastomers based on aromatic disulfide metathesis, Mater. Horiz. 1 (2014) 237–240. https://doi.org/10.1039/C3MH00061C.

[9] D. Montarnal, F. Tournilhac, M. Hidalgo, L. Leibler, Epoxy-based networks combining chemical and supramolecular hydrogen-bonding crosslinks, J. Polym. Sci. Part A Polym. Chem. 48 (2010) 1133–1141. https://doi.org/10.1002/pola.

[10] F. Sordo, S.J. Mougnier, N. Loureiro, F. Tournilhac, V. Michaud, Design of Self-Healing Supramolecular Rubbers with a Tunable Number of Chemical Cross-Links, Macromolecules. 48 (2015) 4394–4402. https://doi.org/10.1021/acs.macromol.5b00747.

[11] F. Sordo, V. Michaud, Processing and damage recovery of intrinsic self-healing glass fiber reinforced composites, Smart Mater. Struct. 25 (2016) 084012. https://doi.org/10.1088/0964-1726/25/8/084012.

[12] Arkema, Reverlink supramolecular technology, (n.d.) 1–8.

[13] Nanocyl, NC7000™–Technical Data Sheet, (2021).

[14] S. Laurenzi, G. de Zanet, M.G. Santonicola, Numerical investigation of radiation shielding properties of polyethylene-based nanocomposite materials in different space environments, Acta Astronaut. 170 (2020) 530–538. https://doi.org/10.1016/j.actaastro.2020.02.027.

[15] NASA, HZETRN2015 User Guide, (2015).

[16] P.M. O'Neill, Badhwar–O'Neill galactic cosmic ray model update based on advanced composition explorer (ACE) energy spectra from 1997 to present, Adv. Sp. Res. 37 (2006) 1727–1733. https://doi.org/10.1016/j.asr.2005.02.001.

[17] R.C. Singleterry, Radiation engineering analysis of shielding materials to assess their ability to protect astronauts in deep space from energetic particle radiation, Acta Astronaut. 91 (2013) 49–54. https://doi.org/10.1016/j.actaastro.2013.04.013.